The Plant Journal (2008) **53**, 287–299 doi: 10.1111/j.1365-313X.2007.03342.x

Loss of the vacuolar cation channel, AtTPC1, does not impair Ca^{2+} signals induced by abiotic and biotic stresses

Stefanie Ranf[1,†], Petra Wünnenberg[2,†], Justin Lee[1], Dirk Becker[3], Marcel Dunkel[3], Rainer Hedrich[3], Dierk Scheel[1] and Petra Dietrich[2,*]

[1]*Leibniz Institute of Plant Biochemistry, Stress and Developmental Biology, Weinberg 3, D-06120 Halle, Germany,*
[2]*University of Erlangen, Institute of Biology, Molecular Plant Physiology, Staudtstrasse 5, D-91058 Erlangen, Germany, and*
[3]*University of Würzburg, Julius-von-Sachs-Institute, Molecular Plant Physiology and Biophysics, Julius-von-Sachs-Platz 2, D-97082 Würzburg, Germany*

Received 23 July 2007; accepted 27 September 2007.
*For correspondence (fax +49 9131 28751; e-mail dietrich@biologie.uni-erlangen.de).
†These authors contributed equally to this paper.

Summary

The putative two-pore Ca^{2+} channel TPC1 has been suggested to be involved in responses to abiotic and biotic stresses. We show that AtTPC1 co-localizes with the K^+-selective channel AtTPK1 in the vacuolar membrane. Loss of *AtTPC1* abolished Ca^{2+}-activated slow vacuolar (SV) currents, which were increased in *AtTPC1*-overexpressing Arabidopsis compared to the wild-type. A Ca^{2+}-insensitive vacuolar cation channel, as yet uncharacterized, could be resolved in *tpc1-2* knockout plants. The kinetics of ABA- and CO_2-induced stomatal closure were similar in wild-type and *tpc1-2* knockout plants, excluding a role of SV channels in guard-cell signalling in response to these physiological stimuli. ABA-, K^+-, and Ca^{2+}-dependent root growth phenotypes were not changed in *tpc1-2* compared to wild-type plants. Given the permeability of SV channels to mono- and divalent cations, the question arises as to whether TPC1 *in vivo* represents a pathway for Ca^{2+} entry into the cytosol. Ca^{2+} responses as measured in aequorin-expressing wild-type, *tpc1-2* knockout and *TPC1*-overexpressing plants disprove a contribution of TPC1 to any of the stimulus-induced Ca^{2+} signals tested, including abiotic stresses (cold, hyperosmotic, salt and oxidative), elevation in extracellular Ca^{2+} concentration and biotic factors (elf18, flg22). In good agreement, stimulus- and Ca^{2+}-dependent gene activation was not affected by alterations in *TPC1* expression. Together with our finding that the loss of *TPC1* did not change the activity of hyperpolarization-activated Ca^{2+}-permeable channels in the plasma membrane, we conclude that TPC1, under physiological conditions, functions as a vacuolar cation channel without a major impact on cytosolic Ca^{2+} homeostasis.

Keywords: SV channel, *TPC1, Arabidopsis thaliana,* vacuole, Ca^{2+} signalling, K^+ homeostasis.

Introduction

AtTPC1, a putative Ca^{2+} channel

In plants, an array of plasma membrane and endomembrane Ca^{2+}-permeable channels has been characterized electrophysiologically (Sanders *et al.*, 2002). In *Arabidopsis thaliana*, a sole member with homology to the voltage-dependent Ca^{2+} channel (Ca_V) family in animal systems exists (Arabidopsis Genome Initiative, 2000). In contrast to these four-domain-containing channels in animals, with a total of 24 transmembrane spans, the Arabidopsis singleton AtTPC1 is composed of only two domains with six transmembrane spans each. Two EF-hand motifs within the cytosolic linker suggest Ca^{2+}-dependent regulation of the protein.

Ca^{2+} transport activity has been postulated for *AtTPC1* and its homologs in tobacco (*NtTPC1*a and *NtTPC1*b), rice (*OsTPC1*) and wheat (*TaTPC1*), after heterologous expression in yeast (Furuichi *et al.*, 2001; Kadota *et al.*, 2004; Kurusu *et al.*, 2004; Wang *et al.*, 2005). NtTPC1s have been characterized as a pathway for Ca^{2+} entry across the plasma membrane in tobacco cells in response to cold shock, sucrose, H_2O_2, salicylic acid, as well as elicitors (Kadota *et al.*, 2004; Kawano *et al.*, 2004; Lin *et al.*, 2005). OsTPC1 has been proposed to localize in the plasma membrane and

to represent a key regulator of elicitor-induced defence responses (Kurusu *et al.*, 2005). TaTPC1 has been reported to reside in the plasma membrane and to function in response to abiotic stresses (Wang *et al.*, 2005). In strong contrast, a vacuolar localization of AtTPC1 was also found (Carter *et al.*, 2004; Peiter *et al.*, 2005). Careful electrophysiological analysis showed that patches excised from *tpc1-2* knockout vacuoles lack cation currents of the slow vacuolar (SV) type, while *AtTPC1*-over-expressing cells exhibited elevated SV channel activities (Peiter *et al.*, 2005).

SV channels in the vacuole

Slowly activating vacuolar (SV) channels open in response to depolarization in the presence of elevated cytosolic Ca^{2+} concentrations (Hedrich and Neher, 1987). Interestingly, in addition to K^+ and Na^+, significant permeability for Ca^{2+} has been documented in the presence of Ca^{2+} as the major charge carrier (Allen and Sanders, 1996; Pottosin *et al.*, 2001; Ward and Schroeder, 1994), thus stimulating an ongoing discussion about the role of SV channels as a source for Ca^{2+}-induced Ca^{2+} release (CICR) across the vacuolar membrane, and subsequent elevation of cytosolic Ca^{2+} concentration (Barkla and Pantoja, 1996; Bewell *et al.*, 1999; Pottosin *et al.*, 1997; Sanders *et al.*, 2002; Ward and Schroeder, 1994, 1997). In guard cells, SV channels may also mediate K^+ efflux during stomatal closure. Thus, the molecular identification of the SV channel as a distantly related member of the voltage-dependent Ca^{2+} channel family (Furuichi *et al.*, 2001) has re-opened the question of its physiological role in K^+ and Ca^{2+} homeostasis.

In this study, we re-evaluated the localization of TPC1, and extended the electrophysiological analysis of *tpc1-2* mutants and *TPC1* over-expressors to the whole-vacuole level, supporting the finding that TPC1 causes SV-type currents in *Arabidopsis thaliana*. Germination and root growth assays, as well as gas exchange measurements, revealed no phenotype in *tpc1-2* mutants under the various conditions tested. The question of whether TPC1 transports Ca^{2+} into the cytosol was addressed using the aequorin Ca^{2+} reporter system. From a detailed comparison of Ca^{2+} responses and Ca^{2+}-dependent gene activation between wild-type, *tpc1-2* knockout and *TPC1*-over-expressing plants, a function in Ca^{2+} release from the vacuole or Ca^{2+} entry via the plasma membrane in response to various biotic and abiotic stresses can be excluded. Together, our results suggest that TPC1 functions as a cation channel without impact on cytosolic Ca^{2+} homeostasis.

Results

Transient co-expression of *AtTPC1* with the vacuolar K^+ channel *AtTPK1* (Czempinski *et al.*, 2002; Schönknecht *et al.*, 2002) N-terminally fused to mRFP1 and mGFP4, respectively, gave rise to fluorescence signals predominantly in the vacuolar membrane and not in the plasma membrane (Figure 1a). These data obtained in onion epidermal cells confirm the results from Arabidopsis mesophyll cells (Peiter *et al.*, 2005), and are in contrast to the localization of AtTPC1, OsTPC1 and TaTPC1 in the plasma membrane of BY-2 and onion epidermal cells (Kawano *et al.*, 2004; Kurusu *et al.*, 2005; Wang *et al.*, 2005).

Loss of TPC1 abolishes Ca^{2+}-activated SV currents

We used the whole-vacuole configuration of the patch–clamp technique to enable the detection of possibly low numbers of active channels in the *tpc1-2* mutant, which could escape observation in excised patches. The results shown in Figure 1(b,c) completely confirm studies on excised patches by Peiter *et al.* (2005). In the wild-type, SV currents in the mesophyll vacuole are able to saturate the patch–clamp amplifier at 20 nA, while no SV currents were recorded in *tpc1-2* mutants under the same conditions. SV currents in *TPC1*-over-expressing vacuoles exceeded those obtained in the wild-type (Figure 1b,c), and emphasize the fact that, under reducing conditions, K^+ release into the cytosol (inward currents in Figure 1b,c) can occur between −50 mV and the Nernst potential for K^+, which is +17 mV under the experimental conditions used (Figure 1b). In excised vacuolar side-in patches, single channels of about 43 pS could be resolved in membranes from wild-type and *TPC1*-over-expressing plants, but were absent from *tpc1-2* patches (Figure 1d). Instantaneous currents, probably due to the activity of fast vacuolar (FV) channels (Hedrich and Neher, 1987; Schönknecht *et al.*, 2002), were not affected by alterations in TPC1 expression (Figure 1e).

When cytosolic Ca^{2+} concentrations were reduced in wild-type samples using 10 mM EGTA in the absence of Ca^{2+}, SV channels remained silent due to their intrinsic Ca^{2+} sensitivity (Hedrich and Neher, 1987), but another time-dependent current component became visible at voltages >140 mV (Figure 2a,c). The lack of SV channels in the *tpc1-2* mutant allowed us to show that the latter conductance is activated independently of the cytosolic Ca^{2+} concentration (Figure 2b,c). We therefore named this channel the Ca^{2+}-insensitive vacuolar channel (CIVC). A single channel conductance of 13 pS further distinguishes CIVC from the SV and FV channels (Figure 2d). Although how CIVC is activated *in vivo* remains unknown, its Ca^{2+} insensitivity, together with a significant Na^+ permeability P_{Na}:P_K of 1.06 ± 0.02 (n = 3), as determined in the *tpc1-2* mutant, suggests that it may complement SV functions under conditions inhibiting Ca^{2+}-sensitive FV channels, i.e. elevated cytosolic Ca^{2+} concentrations (Allen and Sanders, 1996).

In contrast to the tonoplast localization shown here and elsewhere (Carter *et al.*, 2004; Peiter *et al.*, 2005), TPC1 has been proposed to represent a plasma membrane

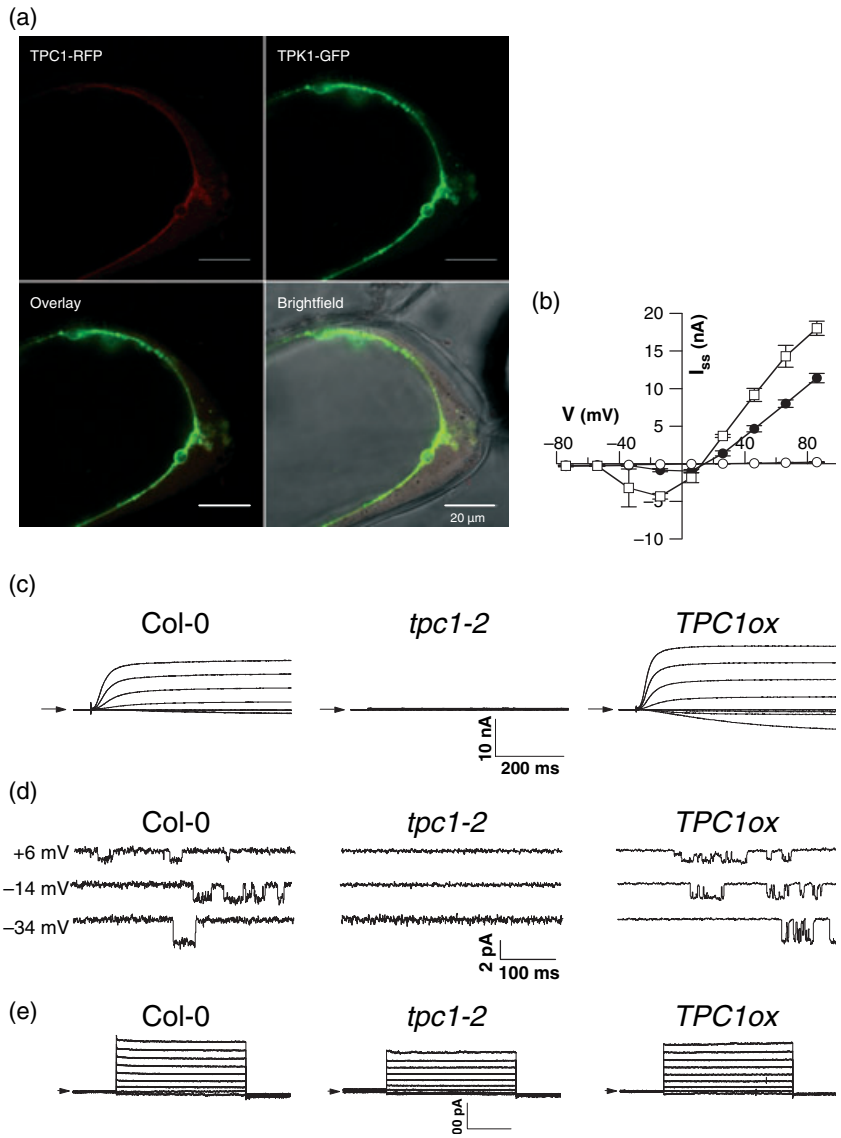

Figure 1. TPC1 functions in the vacuolar membrane.
(a) TPC1–RFP1 (red) and TPK1–GFP (green) fluorescence after transient expression in onion epidermal cells. Bars = 20 µm.
(b) Current–voltage relations of steady-state currents determined from traces as shown in (c), for wild-type (closed circles, n = 13), *tpc1-2* mutants (open circles, n = 9) and *TPC1*-over-expressing plants (open squares, n = 6). Data represent means ± SE.
(c) Whole-vacuolar currents from wild-type (left), *tpc1-2* knockout plants (middle) and *TPC1*-over-expressing plants (right). Currents were elicited by 600 msec test voltages between −74 and +86 mV in 20 mV increments. The presence of SV-type currents in wild-type and *TPC1*-over-expressing samples and their absence in *tpc1-2* were observed without exception.
(d) Single-channel fluctuations in vacuolar side-in patches from vacuoles derived from wild-type (left) and *TPC1*-over-expressing plants (right), but not in those from *tpc1-2* plants (middle). Currents were measured at the voltages indicated. The traces were selected to show openings of a single SV channel and could already be resolved at negative voltages (compare Figures 1b, 2a and 4a,b).
(e) Instantaneous currents in wild-type (left), *tpc1-2* knockout (middle) and *TPC1*-over-expressing plants (right). Currents were measured ≤ 2 min after whole-vacuolar access, before disappearance in Ca^{2+}-containing solutions. Test pulses were applied between −74 and +86 mV in 20 mV increments, starting from a holding potential of −54 mV. Traces are representative for 31 (Col-0), 15 (*TPC1* over-expressors) and 40 (*tpc1-2*) measurements.

Ca^{2+}-permeable channel (Furuichi *et al.*, 2001; Hashimoto *et al.*, 2004; Kadota *et al.*, 2004; Kawano *et al.*, 2004; Kurusu *et al.*, 2004, 2005; Lin *et al.*, 2005; Wang *et al.*, 2005). The dominant plasma membrane Ca^{2+}-permeable channel is activated by hyperpolarization (Grabov and Blatt, 1998; Pei *et al.*, 2000; Stoelzle *et al.*, 2003). In the mesophyll plasma membrane of wild-type and *tpc1-2* mutant plants, we resolved similar cation current amplitudes upon hyperpolarization (Figure 3), excluding the possibility that AtTPC1 mediates this type of Ca^{2+} current.

Root growth and germination of tpc1-2 *mutants*

SV channels in the tonoplast are Ca^{2+}-permeable (Allen and Sanders, 1994; Peiter *et al.*, 2005; Pottosin *et al.*, 2001; Ward and Schroeder, 1994). In the species tested so far, SV channels are equally permeable to K^+ and Na^+, and, accordingly, a value of P_{Na}:P_K of 0.96 ± 0.06 (n = 3) was determined in Arabidopsis under bi-ionic conditions. However, elevated vacuolar Na^+, Cs^+ or Ca^{2+} concentrations shift the voltage dependence of the channel towards depolarized potentials, and reduce the possibility of cation release to the cytoplasm (Figure 4a,b) (Allen and Sanders, 1996; Ivashikina and Hedrich, 2005). Thus, any cation release function of TPC1 depends on the vacuolar and cytosolic cation composition. Under standard growth conditions, *tpc1-2* plants do not develop a characteristic phenotype, and a prediction concerning the exact role of TPC1 in K^+ and/or Ca^{2+} homeostasis is therefore difficult. We tested a putative role of *TPC1* in germination and root growth under various cationic conditions. On agar plates containing K^+ concentrations between 50 µM and 1 mM, germination rates were similar in the wild-type and the *tpc1-2* mutant (Figure 4c). Germination rates were also unaffected by changes in water

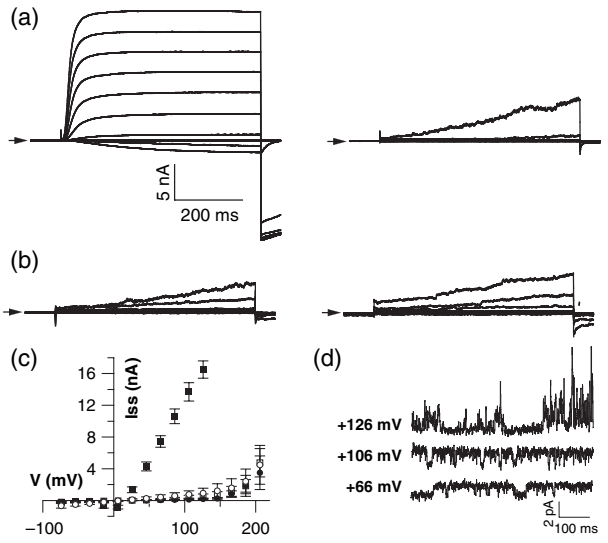

Figure 2. Comparison of Ca^{2+}-sensitive and -insensitive channels in wild-type and *tpc1-2* mutant plants.
(a) Whole-vacuolar currents from wild-type plants recorded before (left) and after (right) exchange of 1 mM Ca^{2+} against 10 mM EGTA in the bath solution.
(b) Whole-vacuolar currents from *tpc1-2* mutants recorded as in (a).
(c) Corresponding current–voltage relations of whole-vacuolar currents in the presence (closed symbols) and from the same cells in the absence (open symbols) of Ca^{2+} for wild-type (squares, $n = 5$) and *tpc1-2* (circles, $n = 3$). Data represent means ± SE.
(d) Single-channel fluctuations for Ca^{2+}-insensitive channels in *tpc1-2* at the indicated voltages.
Currents were measured at test voltages between −74 and +226 mV in 20 mV increments, except for wild-type SV currents in the presence of Ca^{2+}, which were recorded between −74 and +146 mV only [left traces in (a); closed squares in (c)].

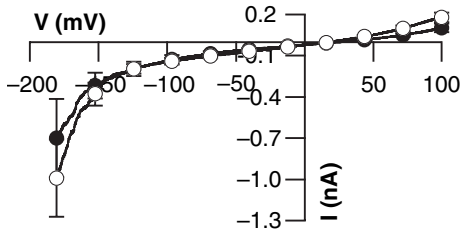

Figure 3. Hyperpolarization-activated Ca^{2+}-permeable channels in the plasma membrane are not affected in the *tpc1-2* mutant.
Current–voltage relations of hyperpolarization-activated channels in wild-type ($n = 11$, closed circles) and *tpc1-2* knockout plants ($n = 20$, open circles). Data represent means ± SE. Currents were elicited in the whole-cell configuration by voltage ramps from +99.5 to −181.5 mV over 2000 msec. Pipette solution: 150 mM K-gluconate, 10 mM EGTA, 3 mM $MgCl_2$, 1 mM MgATP, 10 mM HEPES, pH 7.4/Tris; bath solution: 40 mM Ca-gluconate$_2$, 10 mM MES, pH 5.6/Tris.

potential (0, 5, 10 and 20% PEG 8000, data not shown). No difference in root growth between wild-type and mutant was observed at K^+ concentrations between 5 and 105 mM (Figure 4d). Ca^{2+}-dependent effects on root growth were also equal in wild-type and *tpc1-2* mutant seedlings (Figure 4e). The phytohormone ABA inhibits root growth at 10–50 μM in the wild-type, and this did not differ in the *tpc1-2* mutant (Figure 4f).

Stomatal closure in the tpc1-2 *mutant*

Ca^{2+}-activated SV channels in the tonoplast have been proposed to fulfil a dual function, i.e. K^+ homeostasis and ClCR during stomatal responses to ABA and CO_2, for example (MacRobbie, 2000; Sanders *et al.*, 2002). We used gas exchange measurements in order to follow the kinetics of stomatal movement in the intact leaf. After feeding 100 μM ABA via the petiole, stomatal closure was comparable between *tpc1-2* and wild-type plants (Figure 5a), in agreement with previous observations (Peiter *et al.*, 2005). In response to elevated CO_2 concentration, which, like ABA, induces a rise in the cytoplasmic $[Ca^{2+}]$ (Webb *et al.*, 1996), stomata of wild-type and *tpc1-2* leaves closed with the same kinetics (Figure 5b), indicating that the lack of TPC1 does not interfere with guard-cell Ca^{2+} signalling. The results furthermore show that, if TPC1 does play a role as a K^+ channel, it is not rate-limiting for stomatal closure.

TPC1 does not contribute to Ca^{2+} responses and gene expression induced by abiotic stresses

Cold, mannitol and high salinity, as well as oxidative stress, induce a transient rise in the cytosolic Ca^{2+} concentration, involving Ca^{2+} entry via the plasma membrane, as well as Ca^{2+} release from intracellular stores including the vacuole. Depending on the stimulus, the degree of vacuolar contribution to the Ca^{2+} signature varies, with mannitol and salt stress drawing on the vacuolar Ca^{2+} store to a larger extent than cold and H_2O_2 (Knight *et al.*, 1996, 1997b). We used these abiotic stress stimuli in order to determine the role of TPC1 as a mediator of Ca^{2+} release into the cytosol. Changes in $[Ca^{2+}]_{cyt}$ were resolved using Ca^{2+}-induced cytosolic aequorin luminescence, and showed no difference between wild-type, *tpc1-2* mutant and *TPC1*-over-expressing plants (Figure 6a–d). According to these results, TPC1 does not contribute to the Ca^{2+} release pathway involved in the elevation of $[Ca^{2+}]_{cyt}$ in response to any of the stimuli tested. Elevation of the extracellular Ca^{2+} concentration has been shown to raise the cytosolic Ca^{2+} concentration by drawing on extra- and intracellular Ca^{2+} stores (Han *et al.*, 2003; McAinsh *et al.*, 1995). No difference in cytosolic Ca^{2+} concentration changes between wild-type, *tpc1-2* mutant and *TPC1*-over-expressing plants was measurable in response to 10 mM external Ca^{2+} (Figure 6e).

As a complementary approach, we determined stress-induced gene activation known to require an upstream Ca^{2+} signal. Expression of Δ^1-pyrroline-5-carboxylate synthetase (*P5CS1*), the first enzyme of the proline biosynthesis pathway, was equally induced in wild-type, *tpc1-2* knockout and *TPC1*-over-expressing plants in response to mannitol and

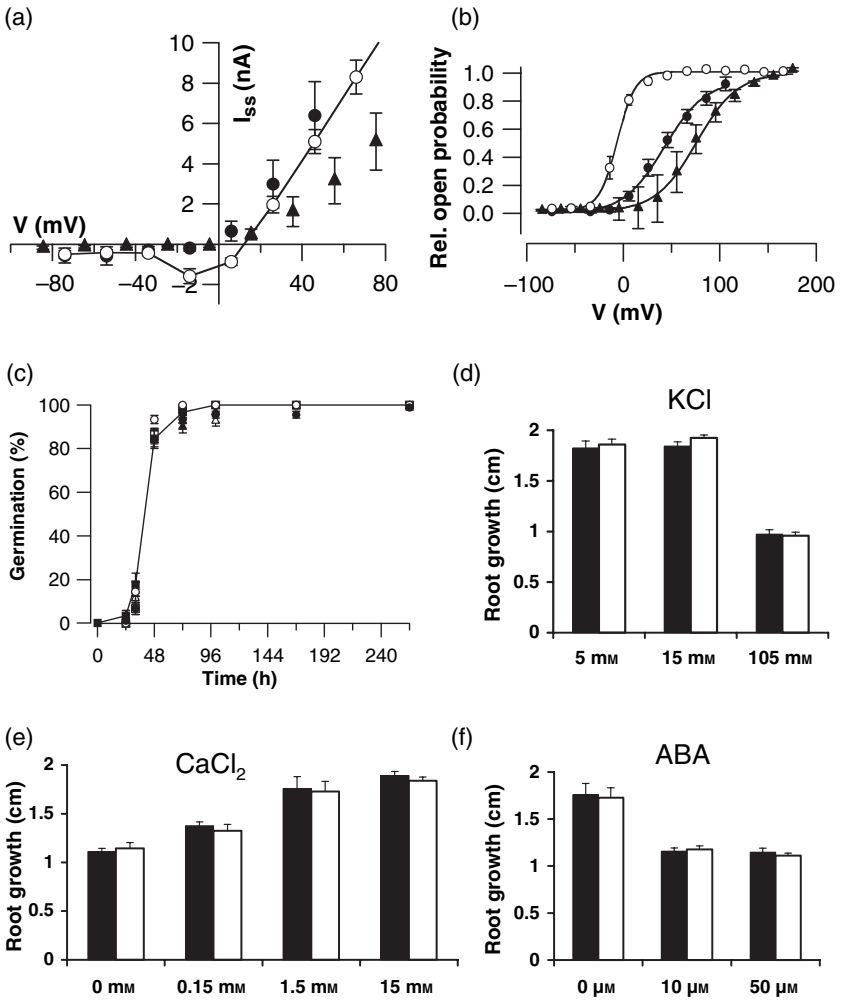

Figure 4. Regulation of wild-type TPC1 activity by cations, and lack of germination and root phenotype in *tpc1-2* mutants.
(a) Steady-state current–voltage relations of wild-type SV currents in the presence of 100 mM K^+ (open circles and line, $n = 6$), Na^+ (closed triangles, $n = 3$) or Cs^+ (closed circles, $n = 5$) on the vacuolar side.
(b) Relative open probabilities of SV channels in the presence of 100 mM K^+ (open circles), Cs^+ (closed circles) or Na^+ (closed triangles) on the vacuolar side. Data were fitted using the Boltzmann equation with half-maximal activation potentials ($V_{½}$) of -6.2 ± 2.6 mV ($n = 6$) for K^+, $+42.6 \pm 5.6$ mV ($n = 4$) for Cs^+, and $+75.6 \pm 16$ mV ($n = 5$) for Na^+.
Data in (a) and (b) represent means ± SE. Whole-vacuolar currents were recorded at test pulses between −74 and +126 mV in 20 mV increments, starting from a holding potential of −54 mV in standard external solution.
(c) Germination of *tpc1-2* (open symbols) versus wild-type seeds (closed symbols) in the presence of various K^+ concentrations. Data represent means ± SE ($n = 6$; total of 90 seeds) for 50 µM (triangle), 500 µM (square) and 1 mM (circle) KCl.
(d–f) Root growth within 4 days after transfer to various K^+ (d), Ca^{2+} (e) and ABA (f) conditions. Data points for wild-type (black bars) and *tpc1-2* (white bars) represent means of seven (±SE; total of 70 plants). Note that 0 mM in (e) corresponds to 50 µM Ca^{2+}.

salt treatment (Figure 6f), confirming that the elevation in $[Ca^{2+}]_{cyt}$ required for gene activation (Knight *et al.*, 1997b) was not altered in *tpc1-2* knockouts or *TPC1* over-expressors. Similarly, Ca^{2+}-dependent induction of *RD29a* by osmotic/drought, cold and salt stresses (Cheong *et al.*, 2003; Kim *et al.*, 2003; Wu *et al.*, 1997) and induction of *GST1* by H_2O_2 (Rentel and Knight, 2004) was comparable in *tpc1-2* knockout, *TPC1*-over-expressing and wild-type plants (Figure 6f).

TPC1 does not contribute to Ca^{2+} responses, oxidative burst or gene expression induced by biotic interactions

Induction of defence responses induced by pathogen-associated molecular patterns (PAMPs) was tested using the bacterial elongation factor Tu N-terminal peptide, elf18, as well as the peptide flg22 that corresponds to the conserved N-terminal part of bacterial flagellin. Both peptides have been shown to act as potent elicitors of the pathogen response, including extracellular alkalinization, oxidative burst and defence gene activation (Felix *et al.*, 1999; Gomez-Gomez *et al.*, 1999; Kunze *et al.*, 2004; Zipfel *et al.*, 2006), while their role in Ca^{2+} signalling during the defence response has not yet been documented. We show here that treatment of leaf discs with elf18 induced a prolonged Ca^{2+} response after a lag phase of about 1 min (Figure 7a), indicating that the peptide is effective in elicitation of Ca^{2+} responses as has been shown for other peptide/protein elicitors, such as pep13 in parsley (Blume *et al.*, 2000; Zimmermann *et al.*, 1997) and cryptogein in tobacco (Lecourieux *et al.*, 2002). A Ca^{2+} signature of similar amplitude and kinetics was induced by treatment with flg22 (Figure 7a). Changes in $[Ca^{2+}]_{cyt}$ are required for downstream defence reactions, including accumulation of reactive oxygen species during the plant–pathogen interaction (Nürnberger and Scheel, 2001). Treatment with the elicitors elf18 and flg22 induced the production of reactive oxygen species such H_2O_2 (Figure 7d, and data not shown), and this production could be completely blocked using the NADPH oxidase inhibitor diphenylene iodonium chloride (DPI, 25 µM), or the Ca^{2+} channel blocker $LaCl_3$ (10 mM), indicating Ca^{2+} dependence of the oxidative burst via NADPH oxidase (data not shown). Accordingly, elf18 led to increased *FRK1*

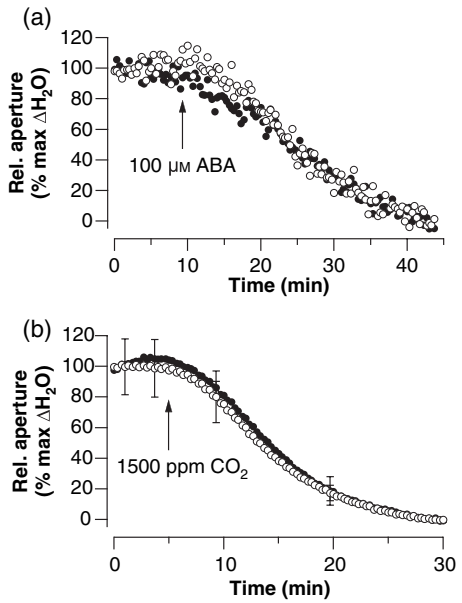

Figure 5. Kinetics of stomatal closure in wild-type and *tpc1-2* mutant plants.
(a) Gas exchange in wild-type (closed circles) and *tpc1-2* knockout plants (open circles) before and after feeding 100 μM ABA (arrow) via the petiole of detached leaves.
(b) Gas exchange in intact leaves of wild-type (closed circles) and *tpc1-2* knockout plants (open circles) after a shift from 50 to 1500 ppm CO_2 (arrow). Data represent means ± SE ($n = 3$ for WT; $n = 5$ for *tpc1-2*). Stomatal movement is expressed as the change in water loss relative to the maximum value.

and *GST1* expression in seedlings (Figure 7c), as was previously shown for the peptide elicitor flg22 (Asai *et al.*, 2002). No difference in the elf18- and flg22-induced Ca^{2+} signature, oxidative burst and marker gene activation was observed between wild-type, *tpc1-2* knockout and *TPC1*-over-expressing plants (Figure 7a,c,d, and data not shown). flg22 induced a growth inhibition of the same extent in *tpc1-2* knockout, *TPC1*-over-expressing and wild-type seedlings (data not shown). H_2O_2 accumulation in leaves infiltrated with an avirulent pathogen, *Pseudomonas syringae* pv. tomato (avrB), was also comparable between wild-type and *tpc1-2* knockout plants (Figure 7e).

We could not detect any Ca^{2+} elevation following the addition of salicylate (Figure 7b), which accumulates during the plant defence response (Nürnberger and Scheel, 2001). It should be noted that the use of free salicylic acid caused some disturbance of the Ca^{2+} homeostasis (data not shown), probably due to non-specific pH effects. However, salicylate induced *PR-1* expression to a similar extent in wild-type, mutant and over-expressing plants (Figure 7c). These results show that salicylate does not induce a rise in cytosolic Ca^{2+} concentration, as has been previously reported using salicylic acid (Lin *et al.*, 2005). In conclusion, by probing for defence-related Ca^{2+} signatures and oxidative burst, as well as downstream gene activation, we could disprove any role of *TPC1* in these plant defence signal transduction pathways.

Finally, taken all together, our analyses covering electrophysiology, *in vivo* measurements of Ca^{2+} signatures and Ca^{2+}-dependent stress responses support our hypothesis that AtTPC1 does not function as a Ca^{2+} channel *in vivo*.

Discussion

AtTPC1 function in pathogen responses

TPC1 is considered to represent a key regulator of elicitor-induced hypersensitive cell death, activation of MAP kinases and defence-related genes in rice and tobacco cells (Kadota *et al.*, 2004; Kurusu *et al.*, 2005). As the elicitor-induced oxidative burst was not suppressed in *Ostpc1* knockout mutants, TPC1 was suggested as a downstream candidate for H_2O_2-induced Ca^{2+} entry. Our data strongly argue against this hypothesis, as Ca^{2+} responses to H_2O_2 at 10 mM (Figure 6d), 100 μM and 25 μM (data not shown) were identical, and downstream expression of *GST1* was not altered (Figure 6f) in wild-type, *tpc1-2* mutant and TPC1-over-expressing Arabidopsis plants. In response to the peptide elicitors elf18 and flg22, a transient rise in $[Ca^{2+}]_{cyt}$ could be demonstrated. Its amplitude and kinetics were similar in wild-type, *tpc1-2* knockout and *TPC1*-over-expressing plants. No reduction or delay in MAPK activation was observed in *tpc1-2* mutant plants treated with either elf18 or flg22, compared to wild-type plants (data not shown). Pathogen-related gene expression and a pathogen-induced oxidative burst occurred independently of the *AtTPC1* expression level. In accordance with our results using bacterial pathogens and elicitors that predominantly induce salicylate signalling, Bonaventure *et al.* (2007) recently reported no difference between wild-type and *tpc1-2* knockout plants in response to infection with the necrotrophic fungus *Botrytis cinerea*, which induces the jasmonate pathway, or in MeJA-induced root growth inhibition. Instead, the effects that they did observe, such as enhanced resistance to *B. cinerea* and elevated oxylipin levels, were seen only in a gain-of-function mutation of *AtTPC1* (*fou2*) that probably leads to mis-regulation of its function – indicating that AtTPC1 *per se* is not involved in these defence processes.

Taken together, this leads us to conclude that TPC1 does not play a crucial role in the signalling pathways of plant defence induced by bacterial or fungal pathogens, nor of the defence-related plant hormones salicylate and jasmonate.

AtTPC1 function in Ca^{2+} homeostasis

In several reports, TPC1 has been suggested to mediate Ca^{2+} entry across the plant plasma membrane in response to cold shock, sucrose, oxidative stress, elicitors and salicylic acid (Furuichi *et al.*, 2001; Kadota *et al.*, 2004; Kawano *et al.*,

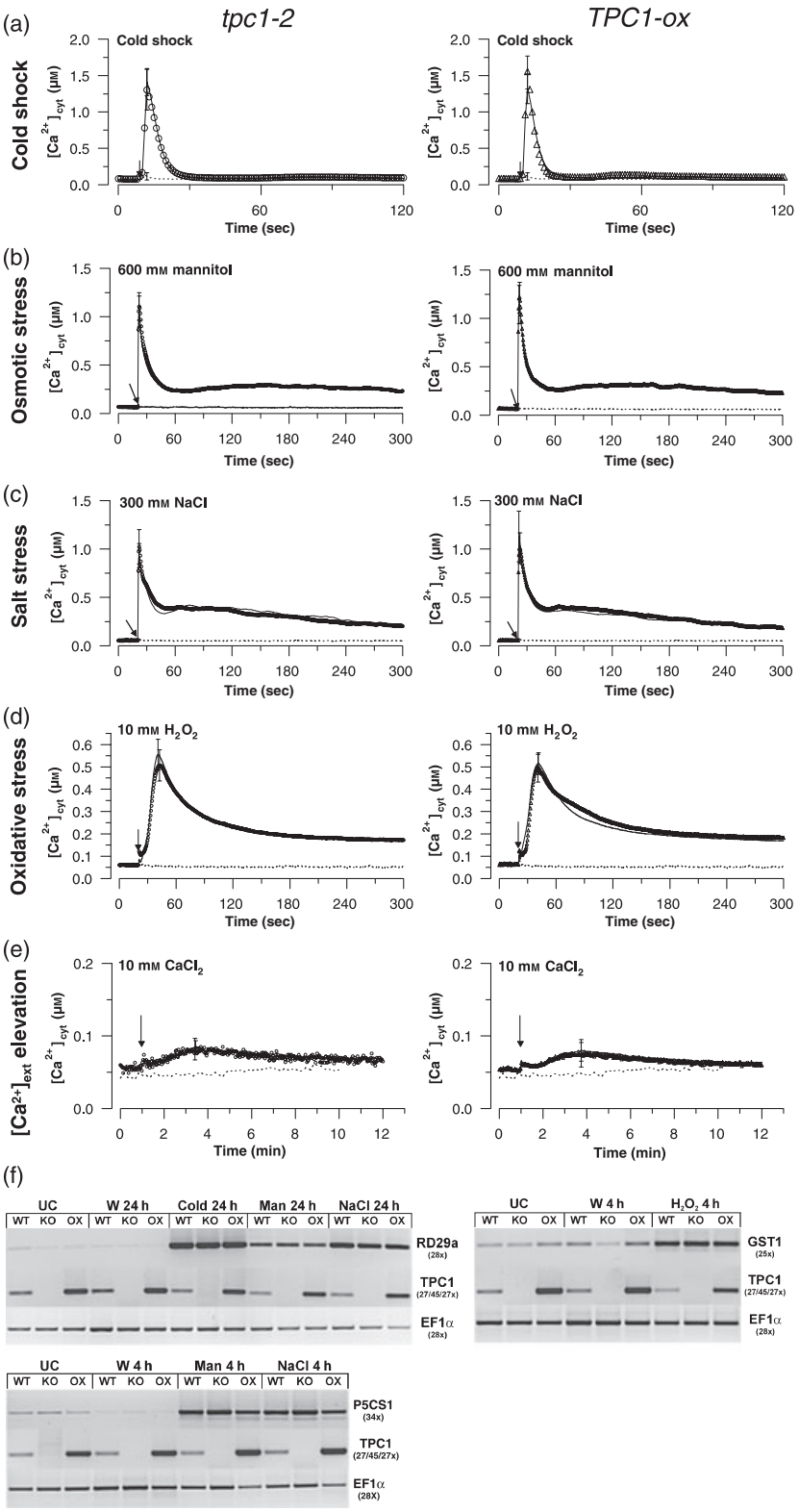

Figure 6. Elevation of cytosolic Ca^{2+} concentration and gene activation induced by abiotic stresses are not altered in *tpc1-2* mutants and *TPC1* over-expressors.
(a) Cold shock was applied by addition of 1 volume ice-cold water.
(b) Osmotic stress was simulated by the addition of 600 mM mannitol.
(c) Ca^{2+} response (300 mM NaCl).
(d) Oxidative stress was induced by 10 mM H_2O_2.
(e) External Ca^{2+} concentration was elevated to 10 mM.
(f) Results from RT-PCR analysis of four stress-related genes: *RD29a* induced by cold, mannitol and NaCl stress, *GST1* induced by oxidative stress, and *P5CS1* induced by mannitol and NaCl stress were visualized in wild-type (WT), *tpc1-2* (KO) and *TPC1*-over-expressing line 10.21 (OX). *EF1α* was used as a constitutive control. Numbers of PCR cycles are indicated in parentheses. UC, untreated control; W, water control; Man, mannitol.
For (a), cytosolic Ca^{2+} concentrations were calculated from relative aequorin luminescence measured in leaf discs using 1 sec integration intervals, for (b)–(d) in seedlings using 0.5 sec integration intervals, and for (e) in leaf discs without lower epidermis using 2 sec integration intervals. Data represent means ± SD, $n \geq 5$. Left graphs: pMAQ2/*TPC1* (WT) (solid lines), pMAQ2/*tpc1-2* (KO) (open circles). Right graphs: pMAQ2 (solid lines), pMAQ2/35S::*TPC1* (OX) (open triangles). Two independent controls were performed (see Experimental procedures for details). Dotted lines represent data obtained upon application of water as a control.

2004; Lin *et al.*, 2005), and across the plasma membrane of yeast cells after heterologous expression (Hashimoto *et al.*, 2004; Wang *et al.*, 2005). In contrast, our results obtained from aequorin luminescence measurements strongly suggest that TPC1 is not involved in the Ca^{2+} response to any of the tested stimuli (Figures 6 and 7). The discrepancy between

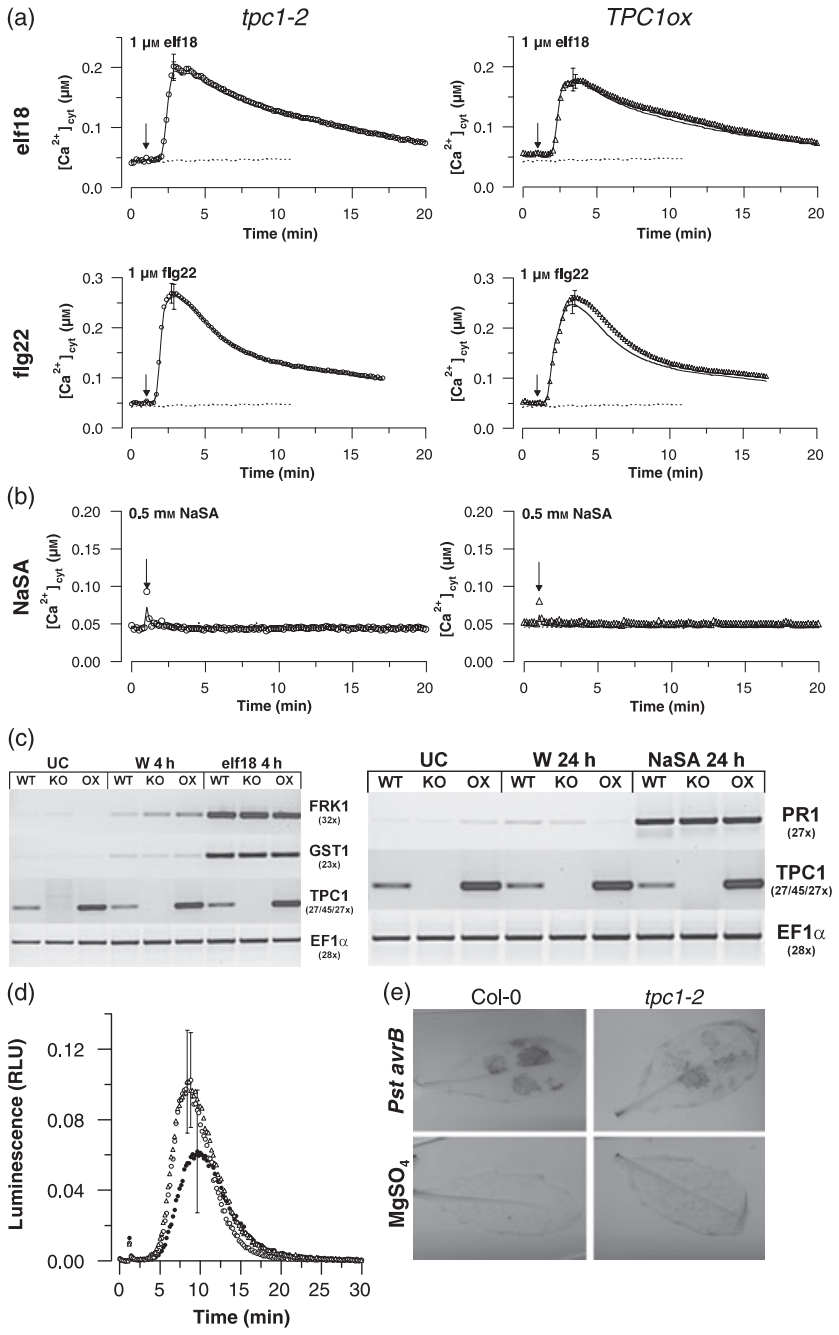

Figure 7. Elevation of cytosolic Ca^{2+} concentration, oxidative burst and gene activation in response to biotic stresses are not altered in *tpc1-2* mutants and *TPC1* over-expressors.
(a) Ca^{2+} response after challenge with the elicitors elf18 or flg22 (1 μM, leaf discs, 10 sec integration interval) following a lag phase of about 1 min in two independent wild-type controls (lines in left and right graphs, respectively), *tpc1-2* (open circles) and *TPC1*-over-expressing lines (open triangles). Data represent means ± SD, $n \geq 5$.
(b) Lack of $[Ca^{2+}]$ elevation after addition of 500 μM sodium salicylate (seedlings, 10 sec integration interval). Data represent means ± SD, $n \geq 5$. Symbols as in (a).
(c) Results from RT-PCR analysis of gene expression induced by biotic stresses: *FRK1* and *GST1* induced by elf18 (10 μM) and *PR-1* by sodium salicylate (500 μM). W, water control; NaSA, sodium salicylate
(d) Oxidative burst in response to treatment with 1 μM elf18 in leaf slices from wild-type (closed circles), *tpc1-2* (open circles) and *TPC1*-over-expressing line 10.21 (open triangles), as determined using a luminol-based assay.
(e) Oxidative burst in response to infection by avirulent *Pseudomonas syringae* pv. tomato (*Pst* avrB) in wild-type (left) and *tpc1-2* knockout plants (right), as determined using DAB staining. Leaves were infiltrated with Pst DC 3000 avrB (upper images) or 10 mM $MgSO_4$ (lower images). Ca^{2+} measurements and RT-PCR experiments were performed as described in Figure 6.

our results and those obtained for aequorin-expressing BY-2 wild-type and *TPC1*-co-suppressing and -over-expressing cell lines may be due to the sensitivity of the aequorin-based method to differences in total luminescence between the plant lines used for comparison. In particular, the free Ca^{2+} level is in a double logarithmic relationship to the aequorin luminescence. For proper quantification and comparability of $[Ca^{2+}]_{cyt}$, it is absolutely necessary to convert these luminescence values into actual $[Ca^{2+}]$ (van Der Luit *et al.*, 1999; Knight *et al.*, 1996, 1997a; Rentel and Knight, 2004). For our studies, we introgressed the pMAQ2 apoaequorin transgene into the *tpc1-2* mutant and *TPC1* over-expressor genetic background to ensure similar aequorin levels. However, we observed a strong reduction of the total aequorin luminescence in all progeny homozygous for the *tpc1-2* mutation. Thus, we carefully selected independent Arabidopsis wild-type lines from the crosses to pMAQ2 to serve as independent controls for knockouts and over-expressors, respectively (see Experimental procedures for details). Our data using lines with comparable total aequorin luminescence and calibrated

$[Ca^{2+}]_{cyt}$ show that, for the stimuli tested, TPC1 apparently does not contribute to Ca^{2+} entry into the cytosol, either from external or internal stores. We cannot, however, exclude a potential role in Ca^{2+} release from the vacuole in very local Ca^{2+} responses, which would escape observation by the cytosolic aequorin reporter.

We demonstrate that hyperpolarization-activated Ca^{2+} currents across the plasma membrane are independent of *TPC1* expression. Instead, we confirm that TPC1 causes SV currents in the vacuolar membrane and show that it co-localizes with AtTPK1, a Ca^{2+}-activated vacuolar K^+-selective (VK) channel (Gobert *et al.*, 2007).

$Ca^{2+}{}_{cyt}$-dependent activation and Ca^{2+} permeability have led to the hypothesis of the SV channel as mediator of CICR from vacuoles. Due to a small open probability in the physiological voltage range of −30 to 0 mV, it has been questioned whether SV channel-mediated CICR occurs *in vivo* (Pottosin *et al.*, 1997). However, potentiation of the Ca^{2+}-dependent activation is induced by cytosolic Mg^{2+} (Pei *et al.*, 1999), revealing a K_d (Ca^{2+}) that is similar to that reported initially in the presence of 1 mM Mg^{2+} (Hedrich and Neher, 1987) and allows gating around 0 mV. Further activating conditions, such as reducing agents and alkaline pH (Carpaneto *et al.*, 1999; Schulz-Lessdorf and Hedrich, 1995), could support channel opening and allow CICR to occur at physiological voltages. According to the results presented here, TPC1 cannot be the source for Ca^{2+} release during CICR, as wild-type-like Ca^{2+} signatures were observed in response to various biotic and abiotic stresses, including elevation of extracellular $[Ca^{2+}]$ in *TPC1* mutants and over-expressors. (Figures 6 and 7). The latter observation is in agreement with the very recent finding that an extracellular Ca^{2+}-induced Ca^{2+} increase exists in guard cells and mesophyll cells, and involves the Ca^{2+}-sensor receptor CAS, which triggers Ca^{2+} release from intracellular stores via second messenger (IP_3) production, and therefore very likely requires ligand-gated rather than voltage-gated Ca^{2+} channel activity (Tang *et al.*, 2007). In guard cells, elevated external Ca^{2+} leads to Ca^{2+} inhibition of plasma membrane K^+ channels (Dietrich *et al.*, 1998; Grabov and Blatt, 1999; Schroeder and Hagiwara, 1989). The Ca^{2+} insensitivity of stomata from the *tpc1-2* mutants (Peiter *et al.*, 2005) therefore does not necessarily indicate alterations in vacuolar Ca^{2+} release, but may suggest changes in cellular K^+ homeostasis. Together, the data presented here strongly suggest that TPC1 functions in Ca^{2+} signalling as a target rather than as a source for Ca^{2+} release from the vacuole.

Under *in vivo* situations, the fractional Ca^{2+} current in the presence of competing K^+ and Na^+ ions has not yet been quantified. The relative Ca^{2+} permeability of TPC1 is only moderate compared to the high Ca^{2+} selectivity of related voltage-dependent Ca_V channels in animal systems (Pottosin *et al.*, 2001). In good agreement, a glutamate residue within the pore region that is responsible for high Ca^{2+} selectivity is conserved between Ca_V channels (Zagotta, 2006), but is missing in both pore domains of AtTPC1 and its homologs in other plant and animal species (Hashimoto *et al.*, 2004). Phylogenetic analyses of ion channel sequences suggest that the divergence of TPC1 from a common ancestor preceded that of Na^+ and Ca^{2+} channels (Anderson and Greenberg, 2001). Given the absence of the latter four-domain Ca^{2+} and Na^+ channels from the Arabidopsis genome, the enigmatic function of the two-pore channel singleton in cation homeostasis requires future research.

Experimental procedures

Plant material and growth conditions

The *AtTPC1* T-DNA mutant line (SALK_145413, *tpc1-2*) was either obtained from D. Sanders (York, UK) (Peiter *et al.*, 2005) or independently retrieved from the SALK collection (Alonso *et al.*, 2003), and plants homozygous for the insertion were identified by PCR, using primer pairs TPC1fw and TPC1rv for verification of the wild-type gene and Lba1 and TPC1rv for the T-DNA insertion (see Table 1). The absence of *TPC1* mRNA in homozygous *tpc1-2* plants was confirmed by RT-PCR using the *TPC1*-specific primers TPC1fw and TPC1rv (see Table 1).

TPC1-over-expressing lines (numbers 5.6 and 10.21) were kindly provided by E. Peiter (York, UK), H. Knight (Durham, UK) and D. Sanders (Peiter *et al.*, 2005), and aequorin-expressing pMAQ2 plants by M. Knight (Durham, UK) and H. Knight. All plant lines used were in the Col-0 background. Seeds were stratified at 4°C for at least 2 days prior to germination. Plants were grown on soil in climate chambers under 8 h:16 h (short day) conditions, or on agar plates under constant light at 22°C.

Electrophysiological recordings

Mesophyll tissue of leaves from 5–10-week-old plants was enzymatically digested (1% BSA, 0.05% pectolyase Y-23 (ICN; http://www.mpbio.com), 0.5% cellulase-R10 (Yakult http://www.yakutt.co.jp), 0.5% macerozyme-R10 (Yakult), 1 mM $CaCl_2$, 10 mM MES, pH 5.6/Tris) at 22°C for 1 h, and washed twice with 400 mM D-sorbitol. Vacuoles were released from the protoplasts by osmotic lysis (10 mM EGTA, 10 mM HEPES, pH 7.4/Tris, sorbitol to 200 mOsM/kg). Vacuolar currents were studied in the whole-vacuolar and vacuolar side-in configuration using an EPC-7 patch–clamp amplifier (List Medical Electronics) and an LIH 1600 interface (HEKA Elektronik; http://www.heka.com). Patch–clamp recordings were performed as described previously (Dietrich and Hedrich, 1998; Hamill *et al.*, 1981). The external (cytoplasmic) solution consisted of 50 mM K-gluconate, 0.2 mM Ca-gluconate$_2$, 0.8 mM $CaCl_2$, 2 mM DTT, 10 mM HEPES pH 7.4/Tris. The pipette (luminal) solution was composed of 100 mM K-gluconate, 2 mM DTT, 10 mM EGTA, 10 mM HEPES pH 7.4/Tris. Solutions were adjusted to an osmolarity of 400 mOsM/kg using D-sorbitol. Any deviations from standard solutions are indicated in the figure legends.

Gas exchange measurements

Wild-type and *tpc1-2* plants were analyzed using a gas exchange fluorescence system (GFS-3000, Heinz Walz GmbH (http://

Table 1 Primers used in this study

Gene	Length (bp)	Primer name	Sequence
AtP5CS1 (At2g39800)	560	P5CS1-F	5′-GGAGGAGCTAGATCGTTCAC-3′
		P5CS1-R	5′-TCAGTTCCAACGCCAGTAGA-3′
AtRD29a (At5g52310)	365	RD29a-F	5′-GAACACTCCGGTCTCTCTGC-3′
		RD29a-R	5′-GCGAATCCTTACCGAGAACA-3′
AtGST1 (At1g02930)	364	GST1-F	5′-TGTCGAGCTCAAAGATGGTG-3′
		GST1-R	5′-GGACTCACCAAGCCTGTGTT-3′
AtFRK1 (At2g19190)	340	FRK1-F	5′-TGAAGGAAGCGGTCAGATTT-3′
		FRK1-R	5′-CTGACTCATCGTTGGCCTCT-3′
AtPR1 (At2g14610)	480	PR1-F	5′-AATTTTACTGGCTATTCTCG-3′
		PR1-R	5′-GTATGGCTTCTCGTTCAC-3′
AtTPC1 (At4g03560)	269	tpc1-2 F2	5′-TGGGGAAACAGCTACCTTCA-3′
		tpc1-2 R2	5′-AGAGCTTTTTGTTCCCAGCA-3′
AtEF1a (At1g07920)	653	EF1a-F	5′-TCACATCAACATTGTGGTCATTGGC-3′
		EF1a-R	5′-TTGATCTGGTCAAGAGCCTCAAG-3′
Other primers used			
		LBa1	5′-TGGTTCACGTAGTGGGCCATCG-3′
		TPC1fw	5′-GGCAGGTTGCCGAGTTTGTC-3′
		TPC1rv	5′-GCAGTAGATACACAGCACGC-3′
		TPC1-fwd	5′-GAGAAGAATGTTGGAGAAAGCCTTTGG-3′
		tpc1-2 rev	5′-CGCAGAAAATGGTCCCTAAA-3′
		Aeq-fwd	5′-ATGAAATATGGTGTGGAAACTGATT-3′
		Aeq-rev	5′-GTTGTCTTGTCATCTCATCAACATC-3′

www.walz.com). Stomatal opening was promoted by superfusion of intact leaves with air containing 50 ppm CO_2, and subsequent stomatal closure was induced by 1500 ppm CO_2. For ABA-induced stomatal closure, detached leaves were opened in the presence of 100 ppm CO_2 in the light, and 100 μM ABA was fed via the petiole. Humidity and light intensities were 11 000 ppm H_2O_{abs}, and 250 μmol m^{-2} sec^{-1} PAR (photosynthetic active radiation), respectively.

Aequorin luminescence measurements

Plants expressing the aequorin apoprotein under control of the 35S promoter in the cytosol were used and were derived from the same homozygous pMAQ2 line (single insertion of aequorin, M. Knight, School of Biological and Biomedical Sciences, Durham University, UK, pers. comm.). Aequorin-expressing *tpc1-2* mutants and *TPC1*-over-expressing lines were generated by crossing of *tpc1-2* and *TPC10.21* with pMAQ2 plants. In case of the knockout, F_2 und F_3 progeny from pMAQ2 × *tpc1-2* crosses homozygous for the *tpc1-2* mutation (knockout) and progenies segregating for the wild-type *TPC1* genotype (as a control, see below) were used. Plants were screened by PCR using primers spanning the T-DNA insertion (tpc1-2 F2/R2, see Table 1), as well as primers for the T-DNA insertion (LBa1) and the *TPC1* gene (tpc1-2 rev), and primers specific for the aequorin cDNA (Aeq-fwd/rev), using genomic DNA. Genotypes were confirmed by RT-PCR using primers spanning the T-DNA insertion (tpc1-2 F2/tpc1-2 rev and tpc1-2 R2) for all lines used. In case of the over-expressor, F_1 progeny from pMAQ2 × *TPC10.21* crosses heterozygous for the 35S::*TPC1* insertion were used, and original pMAQ2 plants were used as a control. Plants were screened by PCR using *TPC1*-specific primers (TPC1 fwd/tpc1-2 rev) spanning eight introns to discriminate between genomic *TPC1* and the inserted *TPC1* cDNA.

We observed a reduction in total aequorin luminescence in all F_2 and F_3 progeny from pMAQ2 × *tpc1-2* crosses tested, and therefore used *TPC1* wild-type genotypes from the same generation as independent controls. Only plants with comparable amounts of total aequorin luminescence were selected for experiments, allowing comparison of the relative luminescence levels and calculated $[Ca^{2+}]_{cyt}$ values.

Leaf discs (diameter 3 mm, 4–8-week-old plants) were cut from mature leaves and floated individually in wells of a 96-well plate on 100 μl H_2O/10 μM native coelenterazine per well (5 mM stock in methanol, Molecular Probes/Invitrogen, http://www.invitrogen.com/) in darkness for at least 4 h for reconstitution. For treatment with external $CaCl_2$, the lower epidermis was removed prior to reconstitution (1 mM MES-KOH, pH 5.7, 100 μM KCl, 10 μM coelenterazine) to allow direct contact of the $CaCl_2$ with the mesophyll tissue. Seedlings were grown axenically on MS agar plates (1 × MS, 1% sucrose, 1% agar), and used when 6–7 days old. Intact seedlings were placed individually in wells of a 96-well plate and reconstituted overnight as described above. Luminescence was measured using a Luminoskan Ascent 2.1 luminometer (Labsystems (http://www.thermo.com)). After 30–60 sec recording, treatment was applied by addition of 50 μl of a threefold concentrated solution in water via an automatic dispenser, and measurements were continued for the indicated time. Controls were performed by addition of an equal volume of water. Remaining aequorin was discharged by automatic injection of 1 volume 2 M $CaCl_2$/20% ethanol, and luminescence recorded for another 8–10 min until values were within 1% of the highest discharge value.

In the case of cold-shock treatment, luminescence was measured in a Lumat LB 9501/16 luminometer (Berthold; http://www.berthold.com). Reconstituted leaf discs were transferred individually to single tubes containing 200 μl H_2O/10 μM coelenterazine, and allowed to recover for at least 15 min from the touch response. Tubes were placed individually into the luminometer chamber, and luminescence recorded at 1 sec integration intervals. After 30 sec, cold shock was applied by manual addition of 1 volume of ice cold water, and measurements were continued for 3 min. Remaining aequorin was discharged as described above.

Relative luminescence values were calculated and converted into actual Ca^{2+} concentrations using the calibration equation below as described in detail by Rentel and Knight (2004):

$$pCa = 0.332588(-\log k) + 5.5593$$

where k is the luminescence counts per sec/total luminescence counts remaining.

Oxidative burst in Arabidopsis leaves

Luminol assay. Reactive oxygen species were assayed by H_2O_2-dependent luminescence of luminol (Gomez-Gomez *et al.*, 1999). Mature Arabidopsis leaves were cut in 1 mm slices and floated overnight on H_2O. Slices were transferred to a 96-well plate (four slices per well) containing 200 μl of H_2O, 200 μM luminol, 2 μg horseradish peroxidase. Luminescence was measured in the Luminoskan Ascent 2.1 luminometer with a 1 sec integration time at 12 sec intervals. After 60 sec, 1 μM elf18 or an equal volume of water was added manually, and luminescence recorded for further 30 min. This assay is not quantifiable and allows only qualitative estimation of H_2O_2 production.

DAB staining. Leaves of wild-type and *tpc1-2* plants were infiltrated with avirulent *P. syringae* pv. tomato Pst *DC3000 avrB* (OD_{600} = 0.2, washed twice in 10 mM $MgSO_4$) and buffer control. Four hours after infection, leaves were transferred to diaminobenzidine solution (1 mg ml^{-1} DAB pH 3.8) and incubated in darkness for 18 h. Chlorophyll was cleared for 10 min in boiling 98% ethanol.

Semi-quantitive RT-PCR experiments

One-week-old seedlings grown as described above were transferred to liquid medium (1 × MS, 1% sucrose) in 24-well plates (two or three seedlings/1 ml per well). Seedlings that were 12–14 days old were treated by exchanging the medium with medium containing 10 μM elf18, 0.5 mM NaSA, 10 mM H_2O_2, 0.6 M mannitol, 0.3 M NaCl or water as control. For cold treatment, the medium was exchanged with ice-cold medium, and seedlings were kept on ice. Whole seedlings were harvested at the time points indicated, frozen in liquid nitrogen and stored at −80°C. Total RNA was prepared using RNeasy plant mini-preps (Qiagen, http://www.qiagen.com/). First-strand synthesis was performed with 1 μg of total RNA (DNase I-treated, Fermentas; http://www.fermentas.de) using 200 U RevertAid M-MuLV reverse transcriptase (Fermentas), oligo$(dT)_{18}$ primer (MWG Biotech; http://www.mwg-biotech.com) and RiboLock RNase inhibitor (Fermentas) according to the manufacturers' instructions. A 0.5 μl aliquot of cDNA was used in a 50 μl PCR reaction containing 2.5 U Taq polymerase (New England Biolabs; http://www.neb.com), HiFi buffer (Fermentas), 1.5 mM $MgCl_2$, 200 μM dNTPs and 200 nM primers (MWG Biotech). Amplification conditions were 1 min at 94°C; *x* cycles of 15 sec at 94°C, 20 sec at 50°C and 45 sec at 72°C, followed by 5 min at 72°C. Optimal PCR cycle numbers determined to be in the non-saturated range have been established previously for each primer pair and are indicated in the text. PCR products were analyzed on 2% TAE agarose gels containing ethidium bromide. Primers were chosen to span at least one intron if possible.

Primers used

The primers used in this study are listed in Table 1.

Root growth measurements and germination assay

Wild-type and *tpc1-2* seedlings were grown on agar plates in climate chambers under a 16 h/8 h light/dark regimen at 22°C. K^+-dependent seed germination was observed for a period of 264 h on modified half-strength MS agar plates in which KNO_3 and KH_2PO_4 had been replaced by NH_4NO_3 and NH_4PO_4. Final $[K^+]$ was adjusted to 50 μM, 500 μM or 1 mM using KNO_3. The medium contained 1.8% K^+-depleted agar (Xu *et al.*, 2006). For root growth measurements, plants were grown on half-strength MS medium containing 1% sucrose and 0.8% agar for 4 days, and then transferred to plates with modified half-strength MS media containing 1% sucrose and 1% purified agar (A7921, Sigma, http://www.sigmaaldrich.com/). For variations in Ca^{2+} contents, 1.5 mM $CaCl_2$ was replaced by 0, 0.15, 1.5 and 15 mM $CaCl_2$, respectively. Note that 0 mM corresponds to approximately 50 μM Ca^{2+}. For ABA-dependent root growth experiments, plants were transferred to half-strength MS plates containing 10 or 50 μM (±) *cis,trans*-ABA in 10 mM KCl and 1.5 mM $CaCl_2$. Root growth within 4 days after transfer was measured using IMAGEJ analysis software (http://rsb.info.nih.gov/ij).

TPC1–GFP construct, transient expression, and confocal fluorescence imaging

For localization of TPC1 in onion epidermal cells, *AtTPC1* cDNA lacking its stop codon was inserted in-frame with *mrfp1* (Campbell *et al.*, 2002) into pPily (Ferrando *et al.*, 2000), creating 2 × 35S-promotor:*TPC1-mrfp1*. In similar fashion, *AtTPK1* cDNA was inserted into pPily in-frame with *mgfp4* (Haseloff *et al.*, 1997), creating 2 × 35S-promotor:*TPK1-mgfp4*. Onion epidermal cells were then co-transfected by biolistic delivery of tungsten particles (tungsten M-17, Bio-Rad, http://www.bio-rad.com/) coated with equal amounts of both plasmids. After 1–2 days, transfected cells were imaged using a Zeiss LSM5 Pascal confocal microscope (http://www.zeiss.com/) in multi-track mode. mGFP4 fluorescence was measured using a 488 nm excitation wavelength and an emission band path of 505–530 nm, while mRFP1 was excited at 543 nm and fluorescence emission was detected using a longpass filter LP560 nm. Images were processed using ZEISS LSM software and ADOBE PHOTOSHOP Elements 2.0.

Acknowledgements

We are grateful to Edgar Peiter (York, UK) Heather Knight (Durham, UK) and Dale Sanders (York, UK) for providing us with two independent *TPC1*-over-expressing lines and the *tpc1-2* mutant line, and Marc Knight (Durham, UK) and Heather Knight for providing the apoaequorin-expressing pMAQ2 line. We would like to thank Oliver Meyerhoff and Katharina Siebke (Heinz Walz GmbH, Effeltrich, Germany) for help with gas exchange equipment and measurements, and Uwe Sonnewald (Erlangen, Germany) for sharing the GFS-3000. We thank Elisabeth Dunkel for technical assistance and Heiner Busch for critical reading of the manuscript. This work was supported by grants from the Deutsche Forschungsgemeinschaft.

References

Allen, G.J. and Sanders, D. (1994) Two voltage-gated, calcium release channels coreside in the vacuolar membrane of broad bean guard cells. *Plant Cell*, **6**, 685–694.

Allen, G.J. and Sanders, D. (1996) Control of ionic currents in guard cell vacuoles by cytosolic and luminal calcium. *Plant J.* **10**, 1055–1069.

Alonso, J.M., Stepanova, A.N., Leisse, T.J. *et al.* (2003) Genome-wide insertional mutagenesis of *Arabidopsis thaliana*. *Science*, **301**, 653–657.

Anderson, P.A. and Greenberg, R.M. (2001) Phylogeny of ion channels: clues to structure and function. *Comp. Biochem. Physiol. B.* **129**, 17–28.

Arabidopsis Genome Initiative (2000) Analysis of the genome sequence of the flowering plant *Arabidopsis thaliana*. *Nature*, **408**, 796–815.

Asai, T., Tena, G., Plotnikova, J., Willmann, M.R., Chiu, W.L., Gomez-Gomez, L., Boller, T., Ausubel, F.M. and Sheen, J. (2002) MAP kinase signalling cascade in *Arabidopsis* innate immunity. *Nature*, **415**, 977–983.

Barkla, B.J. and Pantoja, O. (1996) Physiology of ion transport across the tonoplast of higher plants. *Annu. Rev. Plant Physiol. Plant Mol. Biol.* **47**, 159–184.

Bewell, M.A., Maathuis, F.J.M., Allen, G.J. and Sanders, D. (1999) Calcium-induced calcium release mediated by a voltage-activated cation channel in vacuolar vesicles of red beet. *FEBS Lett.* **458**, 41–44.

Blume, B., Nürnberger, T., Nass, N. and Scheel, D. (2000) Receptor-mediated increase in cytoplasmic free calcium required for activation of pathogen defense in parsley. *Plant Cell*, **12**, 1425–1440.

Bonaventure, G., Gfeller, A., Proebsting, W.M., Hortensteiner, S., Chetelat, A., Martinoia, E. and Farmer, E.E. (2007) A gain-of-function allele of TPC1 activates oxylipin biogenesis after leaf wounding in Arabidopsis. *Plant J.* **49**, 889–898.

Campbell, R.E., Tour, O., Palmer, A.E., Steinbach, P.A., Baird, G.S., Zacharias, D.A. and Tsien, R.Y. (2002) A monomeric red fluorescent protein. *Proc. Natl Acad. Sci. U.S.A.* **99**, 7877–7882.

Carpaneto, A., Cantu, A.M. and Gambale, F. (1999) Redox agents regulate ion channel activity in vacuoles from higher plant cells. *FEBS Lett.* **442**, 129–132.

Carter, C., Pan, S., Zouhar, J., Avila, E.L., Girke, T. and Raikhel, N.V. (2004) The vegetative vacuole proteome of *Arabidopsis thaliana* reveals predicted and unexpected proteins. *Plant Cell*, **16**, 3285–3303.

Cheong, Y.H., Kim, K.N., Pandey, G.K., Gupta, R., Grant, J.J. and Luan, S. (2003) CBL1, a calcium sensor that differentially regulates salt, drought, and cold responses in *Arabidopsis*. *Plant Cell*, **15**, 1833–1845.

Czempinski, K., Frachisse, J.M., Maurel, C., Barbier-Brygoo, H. and Mueller-Roeber, B. (2002) Vacuolar membrane localization of the Arabidopsis 'two-pore' K^+ channel KCO1. *Plant J.* **29**, 809–820.

van Der Luit, A.H., Olivari, C., Haley, A., Knight, M.R. and Trewavas, A.J. (1999) Distinct calcium signaling pathways regulate calmodulin gene expression in tobacco. *Plant Physiol.* **121**, 705–714.

Dietrich, P. and Hedrich, R. (1998) Anions permeate and gate GCAC1, a voltage-dependent guard cell anion channel. *Plant J.* **15**, 479–487.

Dietrich, P., Dreyer, I., Wiesner, P. and Hedrich, R. (1998) Cation sensitivity and kinetics of guard cell potassium channels differ among species. *Planta*, **205**, 277–287.

Felix, G., Duran, J.D., Volko, S. and Boller, T. (1999) Plants have a sensitive perception system for the most conserved domain of bacterial flagellin. *Plant J.* **18**, 265–276.

Ferrando, A., Farras, R., Jasik, J., Schell, J. and Koncz, C. (2000) Intron-tagged epitope: a tool for facile detection and purification of proteins expressed in *Agrobacterium*-transformed plant cells. *Plant J.* **22**, 553–560.

Furuichi, T., Cunningham, K.W. and Muto, S. (2001) A putative two pore channel *At*TPC1 mediates Ca^{2+} flux in *Arabidopsis* leaf cells. *Plant Cell Physiol.* **42**, 900–905.

Gobert, A., Isayenkov, S., Voelker, C., Czempinski, K. and Maathuis, F.J. (2007) The two-pore channel TPK1 gene encodes the vacuolar K^+ conductance and plays a role in K^+ homeostasis. *Proc. Natl Acad. Sci. U.S.A.* **104**, 10726–10731.

Gomez-Gomez, L., Felix, G. and Boller, T. (1999) A single locus determines sensitivity to bacterial flagellin in *Arabidopsis thaliana*. *Plant J.* **18**, 277–284.

Grabov, A. and Blatt, M.R. (1998) Membrane voltage initiates Ca^{2+} waves and potentiates Ca^{2+} increases with abscisic acid in stomatal guard cells. *Proc. Natl Acad. Sci. U.S.A.* **95**, 4778–4783.

Grabov, A. and Blatt, M.R. (1999) A steep dependence of inward-rectifying potassium channels on cytosolic free calcium concentration increase evoked by hyperpolarization in guard cells. *Plant Physiol.* **119**, 277–288.

Hamill, O.P., Marty, A., Neher, E., Sakmann, B. and Sigworth, F.J. (1981) Improved patch-clamp techniques for high-resolution current recording from cells and cell-free membrane patches. *Pflügers Arch.* **391**, 85–100.

Han, S., Tang, R., Anderson, L.K., Woerner, T.E. and Pei, Z.M. (2003) A cell surface receptor mediates extracellular Ca^{2+} sensing in guard cells. *Nature*, **425**, 196–200.

Haseloff, J., Siemering, K.R., Prasher, D.C. and Hodge, S. (1997) Removal of a cryptic intron and subcellular localization of green fluorescent protein are required to mark transgenic *Arabidopsis* plants brightly. *Proc. Natl Acad. Sci. U.S.A.* **94**, 2122–2127.

Hashimoto, K., Saito, M., Matsuoka, H., Iida, K. and Iida, H. (2004) Functional analysis of a rice putative voltage-dependent Ca^{2+} channel, *Os*TPC1, expressed in yeast cells lacking its homologous gene *CCH1*. *Plant Cell Physiol.* **45**, 496–500.

Hedrich, R. and Neher, E. (1987) Cytoplasmic calcium regulates voltage-dependent ion channels in plant vacuoles. *Nature*, **329**, 833–836.

Ivashikina, N. and Hedrich, R. (2005) K^+ currents through SV-type vacuolar channels are sensitive to elevated luminal sodium levels. *Plant J.* **41**, 606–614.

Kadota, Y., Furuichi, T., Ogasawara, Y., Goh, T., Higashi, K., Muto, S. and Kuchitsu, K. (2004) Identification of putative voltage-dependent Ca^{2+}-permeable channels involved in cryptogein-induced Ca^{2+} transients and defense responses in tobacco BY-2 cells. *Biochem. Biophys. Res. Commun.* **317**, 823–830.

Kawano, T., Kadono, T., Fumoto, K., Lapeyrie, F., Kuse, M., Isobe, M., Furuichi, T. and Muto, S. (2004) Aluminum as a specific inhibitor of plant TPC1 Ca^{2+} channels. *Biochem. Biophys. Res. Commun.* **324**, 40–45.

Kim, K.N., Cheong, Y.H., Grant, J.J., Pandey, G.K. and Luan, S. (2003) CIPK3, a calcium sensor-associated protein kinase that regulates abscisic acid and cold signal transduction in *Arabidopsis*. *Plant Cell*, **15**, 411–423.

Knight, H., Trewavas, A.J. and Knight, M.R. (1996) Cold calcium signaling in Arabidopsis involves two cellular pools and a change in calcium signature after acclimation. *Plant Cell*, **8**, 489–503.

Knight, H., Trewavas, A. and Knight, M.R. (1997a) Recombinant aequorin methods for measurement of intracellular calcium in plants. In *Plant Molecular Biology Manual*. Dordrecht: Kluwer Academic Publishers, pp. 1–22.

Knight, H., Trewavas, A.J. and Knight, M.R. (1997b) Calcium signalling in *Arabidopsis thaliana* responding to drought and salinity. *Plant J.* **12**, 1067–1078.

Kunze, G., Zipfel, C., Robatzek, S., Niehaus, K., Boller, T. and Felix, G. (2004) The N terminus of bacterial elongation factor Tu elicits innate immunity in *Arabidopsis* plants. *Plant Cell*, **16**, 3496–3507.

Kurusu, T., Sakurai, Y., Miyao, A., Hirochika, H. and Kuchitsu, K. (2004) Identification of a putative voltage-gated Ca^{2+}-permeable channel (OsTPC1) involved in Ca^{2+} influx and regulation of growth and development in rice. *Plant Cell Physiol.* **45**, 693–702.

Kurusu, T., Yagala, T., Miyao, A., Hirochika, H. and Kuchitsu, K. (2005) Identification of a putative voltage-gated Ca^{2+} channel as a key regulator of elicitor-induced hypersensitive cell death and mitogen-activated protein kinase activation in rice. *Plant J.* **42**, 798–809.

Lecourieux, D., Mazars, C., Pauly, N., Ranjeva, R. and Pugin, A. (2002) Analysis and effects of cytosolic free calcium increases in response to elicitors in *Nicotiana plumbaginifolia* cells. *Plant Cell*, **14**, 2627–2641.

Lin, C., Yu, Y., Kadono, T. *et al.* (2005) Action of aluminum, novel TPC1-type channel inhibitor, against salicylate-induced and cold-shock-induced calcium influx in tobacco BY-2 cells. *Biochem. Biophys. Res. Commun.* **332**, 823–830.

MacRobbie, E.A.C. (2000) ABA activates multiple Ca^{2+} fluxes in stomatal guard cells, triggering vacuolar K^+ (Rb^+) release. *Proc. Natl Acad. Sci. U.S.A.* **97**, 12361–12368.

McAinsh, M.R., Webb, A.A.R., Taylor, J.E. and Hetherington, A.M. (1995) Stimulus-induced oscillations in guard cell cytosolic free calcium. *Plant Cell*, **7**, 1207–1219.

Nürnberger, T. and Scheel, D. (2001) Signal transmission in the plant immune response. *Trends Plant Sci.* **6**, 372–379.

Pei, Z.M., Ward, J.M. and Schroeder, J.I. (1999) Magnesium sensitizes slow vacuolar channels to physiological cytosolic calcium and inhibits fast vacuolar channels in fava bean guard cell vacuoles. *Plant Physiol.* **121**, 977–986.

Pei, Z.M., Murata, Y., Benning, G., Thomine, S., Klusener, B., Allen, G.J., Grill, E. and Schroeder, J.I. (2000) Calcium channels activated by hydrogen peroxide mediate abscisic acid signalling in guard cells. *Nature*, **406**, 731–734.

Peiter, E., Maathuis, F.J., Mills, L.N., Knight, H., Pelloux, J., Hetherington, A.M. and Sanders, D. (2005) The vacuolar Ca^{2+}-activated channel TPC1 regulates germination and stomatal movement. *Nature*, **434**, 404–408.

Pottosin, I.I., Tikhonova, L.I., Hedrich, R. and Schoenknecht, G. (1997) Slowly activating vacuolar channels cannot mediate Ca^{2+}-induced Ca^{2+} release. *Plant J.* **12**, 1387–1398.

Pottosin, I.I., Dobrovinskaya, O.R. and Muniz, J. (2001) Conduction of monovalent and divalent cations in the slow vacuolar channel. *J. Membr. Biol.* **181**, 55–65.

Rentel, M.C. and Knight, M.R. (2004) Oxidative stress-induced calcium signaling in *Arabidopsis*. *Plant Physiol.* **135**, 1471–1479.

Sanders, D., Pelloux, J., Brownlee, C. and Harper, J.F. (2002) Calcium at the crossroads of signaling. *Plant Cell*, **14**, S401–S417.

Schönknecht, G., Spoormaker, P., Steinmeyer, R., Brüggeman, L., Ache, P., Dutta, R., Reintanz, B., Godde, M., Hedrich, R. and Palme, K. (2002) KCO1 is a component of the slow-vacuolar (SV) ion channel. *FEBS Lett.* **511**, 28–32.

Schroeder, J.I. and Hagiwara, S. (1989) Cytosolic calcium regulates ion channels in the plasma membrane of *Vicia faba* guard cells. *Nature*, **338**, 427–430.

Schulz-Lessdorf, B. and Hedrich, R. (1995) Protons and calcium modulate SV-type channels in the vacuolar-lysosomal compartment: channel interaction with calmodulin inhibitors. *Planta*, **197**, 655–671.

Stoelzle, S., Kagawa, T., Wada, M., Hedrich, R. and Dietrich, P. (2003) Blue light activates calcium-permeable channels in *Arabidopsis* mesophyll cells via the phototropin signaling pathway. *Proc. Natl Acad. Sci. U.S.A.* **100**, 1456–1461.

Tang, R.H., Han, S., Zheng, H., Cook, C.W., Choi, C.S., Woerner, T.E., Jackson, R.B. and Pei, Z.M. (2007) Coupling diurnal cytosolic Ca^{2+} oscillations to the CAS-IP3 pathway in Arabidopsis. *Science*, **315**, 1423–1426.

Wang, Y.-J., Yu, J.-N., Chen, T., Zhang, Z.-G., Hao, Y.-J., Zhang, J.-S. and Chen, S.-Y. (2005) Functional analysis of a putative Ca^{2+} channel gene *TaTPC1* from wheat. *J. Exp. Bot.* **56**, 3051–3060.

Ward, J.M. and Schroeder, J.I. (1994) Calcium-activated K^+ channels and calcium-induced calcium release by slow vacuolar channels in guard cell vacuoles implicated in the control of stomatal closure. *Plant Cell*, **6**, 669–683.

Ward, J.M. and Schroeder, J.I. (1997) Roles of ion channels in initiation of signal transduction in higher plants. In *Molecular and Cell Biology Updates: Signal Transduction in Plants* (Aducci, P., ed.). Basel: Birkhäuser Verlag, pp. 1–22.

Webb, A.A.R., McAinsh, M.R., Mansfield, T.A. and Hetherington, A.M. (1996) Carbon dioxide induces increases in guard cell cytosolic free calcium. *Plant J.* **9**, 297–304.

Wu, Y., Kuzma, J., Marechal, E., Graeff, R., Lee, H.C., Foster, R. and Chua, N.H. (1997) Abscisic acid signaling through cyclic ADP-ribose in plants. *Science*, **278**, 2126–2130.

Xu, J., Li, H.D., Chen, L.Q., Wang, Y., Liu, L.L., He, L. and Wu, W.H. (2006) A protein kinase, interacting with two calcineurin B-like proteins, regulates K^+ transporter AKT1 in *Arabidopsis*. *Cell*, **125**, 1347–1360.

Zagotta, W.N. (2006) Membrane biology: permutations of permeability. *Nature*, **440**, 427–429.

Zimmermann, S., Nürnberger, T., Frachisse, J.-M., Wirtz, W., Guern, J., Hedrich, R. and Scheel, D. (1997) Receptor-mediated activation of a plant Ca^{2+}-permeable ion channel involved in pathogen defense. *Proc. Natl Acad. Sci. U.S.A.* **94**, 2751–2755.

Zipfel, C., Kunze, G., Chinchilla, D., Caniard, A., Jones, J.D., Boller, T. and Felix, G. (2006) Perception of the bacterial PAMP EF-Tu by the receptor EFR restricts Agrobacterium-mediated transformation. *Cell*, **125**, 749–760.

